Journal of Nuclear Materials 394 (2009) 46–51

Contents lists available at ScienceDirect

Journal of Nuclear Materials

journal homepage: www.elsevier.com/locate/jnucmat

Uniaxial creep response of Alloy 800H in impure helium and in low oxygen potential environments for nuclear reactor applications

K. Natesan, P.S. Shankar *

Argonne National Laboratory, 9700 S. Cass Ave., Argonne, IL 60439, USA

ARTICLE INFO

Article history:
Received 30 March 2009
Accepted 5 August 2009

ABSTRACT

Studies were conducted on the creep behavior of Alloy 800H in impure helium and in a 1%CO–CO_2 environment. At relatively low applied stresses and at low temperatures, the presence of methane in helium reduced the rupture strain significantly while increasing the rupture life relative to the behavior in pure helium. The degradation in rupture strain is due to the occurrence of cleavage fracture in the He + CH_4 environment; this explanation is also supported by high activation energy (Q = 723 kJ/mol) for creep in He + CH_4. At higher applied stresses and also at higher temperatures, creep-rupture behavior in He and He + CH_4 was similar. Creep response in pure He and in CO–CO_2 follows a dislocation climb-controlled power-law behavior whereas that in He + CH_4 has a different behavior as indicated by the high stress exponent (n = 9.8). The activation energy for creep in pure He was 391 kJ/mol and in CO–CO_2 was 398 kJ/mol, and appeared to be independent of stress in both environments. On the other hand, in He + CH_4, the activation energy (Q = 723 kJ/mol) seems to be dependent on stress.

1. Introduction

The Next Generation Nuclear Plant (NGNP), which is based on advanced high temperature gas reactor concept with emphasis on production of both electricity and hydrogen, involves helium as the coolant and a closed-cycle gas–turbine or a steam turbine for power generation with a core outlet/gas–turbine inlet temperature of 850–950 °C [1]. The concept for the very high temperature reactor (VHTR) can be a system based on the prismatic block of the gas–turbine-modular helium reactor developed by a consortium led by General Atomics in the US or based on the Pebble Bed Modular Reactor (PBMR) design developed by ESKOM of South Africa and British Nuclear Fuels of UK. In the VHTR concept, helium is used as a coolant, which upon exiting from the reactor core is used to drive the turbine directly or indirectly by heating air or nitrogen that drive the turbines [1]. In both NGNP and VHTR concepts, the primary helium coolant is expected to reach temperatures of 850–950 °C. Thus, the structural materials for use in the core, heat exchangers, control rods, and turbine sections should possess adequate mechanical performance up to ≈1000 °C, in nominally impure helium environments.

Although gaseous helium is inert by itself, past studies [2–8] have shown that small amounts (in parts per million concentrations) of contaminants like H_2, H_2O, CH_4, O_2, CO_2 present in the helium gas can significantly affect the scaling and morphology of surface regions of the metallic components at high operating temperatures, thereby affecting long-term mechanical properties like creep. Therefore, it is necessary to select, evaluate, and develop/modify metallic materials that have improved creep resistance in impure helium environments containing the aforementioned impurities.

Alloy 800H is a Fe–32Ni–20Cr austenitic alloy with a minimum 0.05 wt.% carbon content and a coarse grain structure (ASTM No. 5 or coarser). This alloy must be solution-annealed at ≈1093 °C, has stable austenitic structure, and is intended for use at temperatures >593 °C. Both the high carbon content and the high solution-anneal temperature promote a large stable grain size, which provides better creep resistance. The material is free of precipitates in the solution-annealed condition. After long times at a service temperatures of >550 °C, γ′ precipitates tend to form. These precipitates can reduce the creep ductility of the alloy [9]. To minimize the decrease in creep ductility, the volume fraction of γ′ precipitates is controlled by specifying a concentration limit of ≈0.8 wt.% for the Al + Ti content in the alloy. This alloy is approved for use up to 760 °C under ASME Code Section III Subsection NH for nuclear applications, and is a candidate for control rods and heat exchangers of the helium-cooled reactors. Alloy 800H is the primary candidate for use as control rods in the Pebble Bed Modular Reactor design concept for the NGNP [10]. Past studies [2–8,11] on the creep-rupture of Alloy 800H in helium were aimed at steam-cycle and process-nuclear-heat based gas cooled reactors. It is however, necessary to evaluate the creep-rupture behavior of Alloy 800H under gas–turbine conditions because the level of impurities (and

* Corresponding author. Tel.: +1 630 252 5103; fax: +1 630 252 3604.
E-mail address: natesan@anl.gov (P.S. Shankar).

0022-3115/$ - see front matter © 2009 Elsevier B.V. All rights reserved.
doi:10.1016/j.jnucmat.2009.08.004

thus the oxygen potential) in helium in the steam-cycle and the gas–turbine cycle are different [4,8]. For example, the oxygen potential is expected to be lower in the gas–turbine concept as compared to the steam generating systems. Therefore, the objective of the present study was to evaluate the uniaxial creep behavior of Alloy 800H in helium containing low levels of impurities and in other low oxygen potential environments.

2. Materials and methods

The creep behavior of Alloy 800H, with a composition in wt.%: C 0.08, Cr 20.1, Ni 31.7, Mn 1.0, Si 0.2, Mo 0.3, Al 0.4, Ti 0.31, Fe balance, was evaluated at several temperatures and applied stresses in pure helium and in helium containing small volume additions of methane impurity. The nominal composition of pure helium was He – 99.999%, O_2 <1 ppm, H_2O <2 ppm, and total hydrocarbons <1 ppm. A helium test facility consisting of a mass spectrometer and a micro-gas chromatograph was built to control and monitor the impurity levels of oxygen and/or methane in the exposure environment. The spectrometer and the chromatograph were calibrated for continuous measurement of gas phase impurities in helium. Care was taken to ensure that the impurity levels were controlled and maintained at required ppm levels throughout the entire duration of the creep tests. In addition to tests in helium, creep tests were also conducted in 1%CO–CO_2 environment that represents low oxygen potential (without hydrocarbon) in the exposure environment. The carbon activity values established by this gas mixture are very low (in the range from 4×10^{-5} to 2.1×10^{-6} in the temperature range from 750 °C to 927 °C) and should not result in carburization of Alloy 800H during creep testing.

The Alloy 800H was creep tested in environments consisting of pure helium (He) and in helium containing 675 vppm methane (hereafter referred to as He + CH_4) at 750 °C and 843 °C at stresses ranging from 27.6 MPa to 103.4 MPa. Creep tests in the low oxygen potential 1%CO–CO_2 environment were conducted at 750–927 °C. All the creep tests were performed at 1 atm total pressure. The aim of these tests was to evaluate the influence of impurities in helium on the rupture life, rupture strain, and minimum creep rate, $\dot{\varepsilon}$. The effect of impurity content in He on the stress and temperature dependence was also evaluated. Creep failure modes and mechanisms were characterized and correlated with the macroscopic creep response.

The creep tests were performed according to ASTM E139-96 on polished cylindrical specimens of gage length 19.1 mm and 3.8 mm diameter using direct-load creep machines. The specimens were loaded at constant rate to full load at the test temperature. Creep strain in the specimens was measured using a linear variable differential transducer (LVDT) whose sensitivity was ≈5 μm. The LVDT was calibrated before start of each test to ensure consistency in strain measurements. The creep elongation was continuously recorded by a data acquisition system attached to the test facility. After specimen failure, creep strain vs. time curves were generated using the acquired creep elongation and time data. Subsequently, minimum creep rate, $\dot{\varepsilon}$, was extracted from the experimental creep curves using a linear least squares analysis.

3. Results and discussion

Fig. 1 shows the creep strain-rupture life behavior of Alloy 800H at 843 °C in pure helium environment at different applied stresses. At 27.6 MPa, the sharp increase in creep strain after ≈7500 h is due to an increase in applied stress (from 27.6 MPa to 41.4 MPa) that was done to induce specimen failure. Table 1 lists the creep-rupture data of Alloy 800H tested at 750 °C and 843 °C in environments of pure helium and in helium containing 675 vppm methane. Calculated values for the minimum creep rate, $\dot{\varepsilon}$, are also shown in the table. As expected, in both the environments and at both temperatures, the rupture life decreases and the rupture strain increases with an increase in applied stress. The creep-rupture response at 750 °C in pure helium is similar to that observed by Roberts [12] at 760 °C in helium. It should be noted that the work of Roberts [12] and other studies on 800H [6,7,13] were performed in helium environments typical of steam-cycle reactors. Lee's [6] work at 760 °C was performed at stresses less than 55.2 MPa that prevents a direct comparison with the current results. However, the creep rates observed therein appear to be of the same order of magnitude as those in the present study.

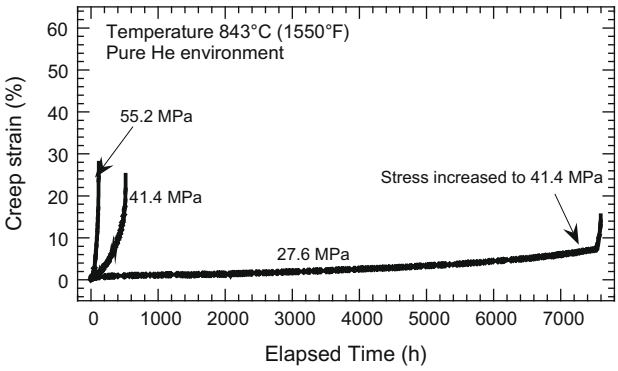

Fig. 1. Creep strain vs. time for Alloy 800H at 843 °C in pure helium environment.

Figs. 2 and 3 show the creep strain-rupture life behavior in He + CH_4 environment at 750 °C and 843 °C respectively, illustrating the effect of methane on the rupture life and rupture strain. It is evident that at relatively low applied stresses at 750 °C, the rupture life is much greater and the rupture strain is significantly lower in specimens tested in He + CH_4 than those tested in pure helium. For example, at 750 °C and at an applied stress of 68.9 MPa, the rupture life is 3396 h and the rupture strain is 14.5% in He + CH_4 whereas the life is 1030 h and the corresponding rupture strain is 28.75% in pure helium. On the other hand, at higher applied stresses, the rupture strains and rupture life are similar in both environments and at both temperatures as seen in Table 1. In contrast to the results of the present study, Schubert et al. [7] reported negligible difference in the rupture life and rupture strain of Alloy 800H in helium and in methane-reforming process gas at 800 °C and 950 °C in the stress range 6–80 MPa. Since the process gas composition used in that study [7] is not measured but only calculated, it is not possible to compare our results with theirs to explain the difference in creep behavior.

Fig. 4 shows the creep curves of Alloy 800H in 1%CO–CO_2 environment at various temperatures. Table 2 shows the corresponding creep-rupture data. The equilibrium pO_2 values at different temperatures are also shown in the table. The low-pO_2 values are representative of the dry environments expected in the gas–turbine systems. It should be mentioned that the pO_2 levels in pure helium were even lower (3–4 orders of magnitude) than in the 1%CO–CO_2 environment. As seen in Tables 1 and 2, the creep behavior in the 1%CO–CO_2 environment and in pure helium is similar. The similar creep behavior in the two environments can be attributed to the very low equilibrium pO_2 levels.

3.1. Temperature and stress dependence of creep

The minimum creep rate, $\dot{\varepsilon}$, is usually expressed as [14,15],

$$\dot{\varepsilon} = A\sigma^n \exp\left(\frac{-Q}{RT}\right) \quad (1)$$

Table 1
Creep data for Alloy 800H at 750 °C and 843 °C in helium with and without methane.

Environment	Temperature (°C)	Applied stress (MPa)	Rupture life (h)	Rupture strain (%)	Minimum creep rate (s^{-1})
Pure He	750	68.9	1030	28.8	3×10^{-8}
	–	89.6	491	40.8	7.7×10^{-8}
	–	103.4	208	54.9	2.4×10^{-7}
He – 675 vppm CH_4	750	68.9	3396	14.5	3×10^{-9}
	–	89.6	332	44.3	1.3×10^{-7}
Pure He	843	27.6	7598[a]	15.4	1×10^{-9}
	–	41.4	516	25.1	3.1×10^{-8}
	–	55.2	115	27.8	1.9×10^{-7}
He – 675 vppm CH_4	843	41.4	406	17.6	7.7×10^{-8}
	–	55.2	105	30.9	4.3×10^{-7}

[a] Applied stress increased to 41.4 MPa after ≈7500 h to induce specimen failure.

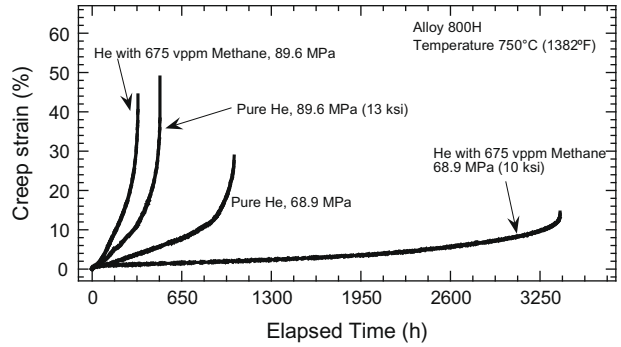

Fig. 2. Effect of methane on the creep-rupture behavior of Alloy 800H at 750 °C.

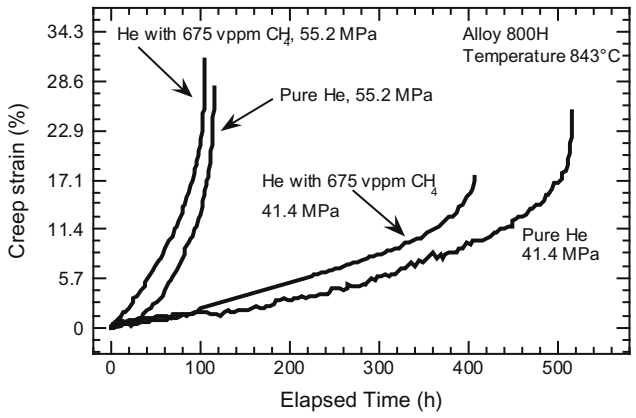

Fig. 3. Effect of methane on the creep-rupture behavior of Alloy 800H at 843 °C.

where σ is the applied stress, n is the stress exponent, Q is the activation energy for creep mechanism, A is a constant, R is the universal gas constant, and T the absolute temperature. The value of n and Q can be estimated by a multiple regression analysis of the creep data at different temperatures and stresses. Based on the data in Tables 1 and 2, the regression analysis yielded values of $n = 6.9$ and $Q = 391$ kJ/mol for tests in He, $n = 5.6$ and $Q = 398$ kJ/mole for tests in 1%CO–CO_2, and $n = 9.8$ and $Q = 723$ kJ/mol for tests in He + CH_4 environments. The values of the stress exponent in He and CO–CO_2 environments suggest a dislocation climb-controlled behavior [14,16] whereas the high value of n in the He + CH_4 environment indicates a different creep mechanism. Higher values of n typically occurs when the stresses are very high resulting in an exponential creep behavior [17] or it can occur at relatively low stresses with a very high activation energy for creep (more than 2–3 times the activation energy for self-diffusion) [18].

Provided there is a weak dependence of activation energy on stress, the stress dependence of creep can be approximately assessed using Norton's relationship [19],

$$\dot{\varepsilon} = A\sigma^n \tag{2}$$

Usually, most metals and alloys in the stress range $10^{-4} < \sigma/E < 10^{-2}$ are observed to follow Eq. (2) with $n = 4$–7 [16,20,21]. Using the data listed in Tables 1 and 2, the creep rate is plotted as a function of applied stress and is shown in Fig. 5. The values of the stress exponent, n calculated from the slope of the best-fit straight lines are also shown in the figure. In pure He, the n-values obtained at 750 °C ($n = 4.9$) and 843 °C ($n = 7.6$) suggest a power-law dislocation climb-controlled behavior. These n -values are roughly close to the n-value ($n = 6.9$) obtained by the regression analysis. The similar n-values (and thus similar creep-mechanisms) estimated by Eqs. (1) and (2) suggests that Eq. (2) provides a good approximation for the stress dependence of creep at a given temperature in pure helium environment. In other words, it can be inferred that the activation energy is weakly dependent on stress in pure helium environment. A similar reasoning, i.e., similar n-values estimated by Eqs. (1) and (2), can be used to infer that the activation energy is independent of stress in the CO–CO_2 environment. In contrast to He and CO–CO_2 environments, $n = 9.8$ obtained from the regression analysis for the tests in He + CH_4 is very different than the n -values ($n = 6.0$ at 843 °C, and $n = 14.4$ at 750 °C) in Fig. 5. This suggests that the minimum creep rate does not independently depend on stress and activation energy in the He + CH_4 environment. In other words, there appears to be a dependence of activation energy on stress in He + CH_4 environment.

For a dislocation creep mechanism, as observed in He and CO–CO_2 environments, the activation energy for creep is expected to be same as that for lattice self-diffusion. From the results of the multiple regression analysis, the activation energies in pure He ($Q = 391$ kJ/mole) and in CO–CO_2 environment ($Q = 398$ kJ/mole) are slightly higher than the activation energy for self-diffusion, Q_{sd} in pure γ-iron ($Q_{sd} \approx 270$ kJ/mol) [22]. Higher apparent activation energy than Q_{sd} has been observed in solid solution alloys exhibiting n ≈5 and can be expected when the temperature dependence of elastic modulus and effect of friction stress are not considered [23,24]. In the He + CH_4 environment, the value of Q ($Q = 723$ kJ/mol) is more than twice the activation energy for self-diffusion in γ-iron. The very high activation energy suggests a different creep mechanism, in concurrence with the high stress exponent observed in this environment. A high activation energy can arise at high stresses where dislocation glide controls creep or it can also arise at relatively lower stresses and temperatures

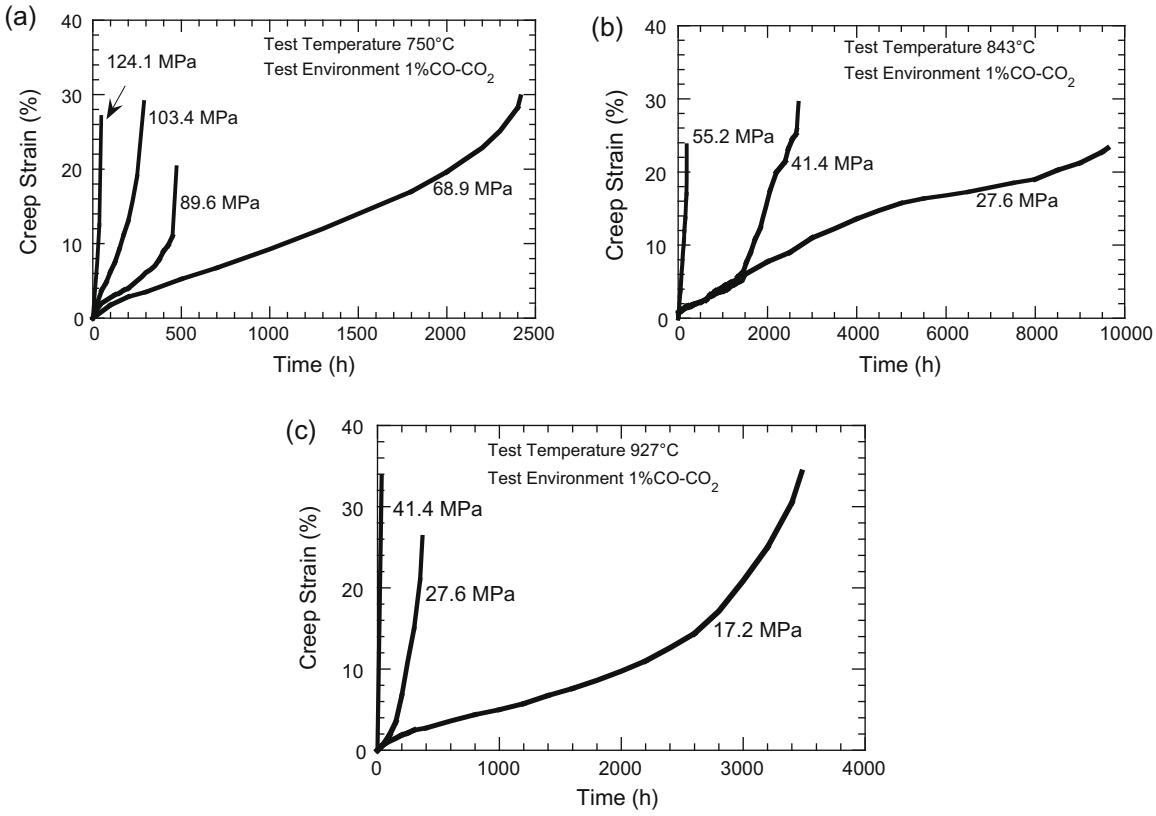

Fig. 4. Creep behavior of Alloy 800H in 1%CO–CO_2 environment at various temperatures (a) 750 °C, (b) 843 °C, and (c) 927 °C.

Table 2
Creep behavior of Alloy 800H in low-pO_2 (1%CO–CO_2) environment.

Temperature (°C)	pO_2 (atm)	Applied stress (MPa)	Rupture life (h)	Rupture strain (%)	Minimum creep rate (s^{-1})
750	1.9×10^{-16}	68.9	2416	29.8	2.9×10^{-8}
		89.6	473	20.3	5.8×10^{-8}
		103.4	269	29.0	1.8×10^{-7}
		124.1	47	27.0	8.3×10^{-7}
843	4.8×10^{-14}	27.6	9620	23.3	1.0×10^{-8}
		41.4	2697	29.5	1.2×10^{-8}
		55.2	191.7	23.7	2.1×10^{-7}
		41.4	516	25.1	3.1×10^{-8}
927	3.4×10^{-12}	17.2	3482	34.3	1.4×10^{-8}
		27.6	370	26.3	6.4×10^{-8}
		41.4	35	33.8	2.7×10^{-6}

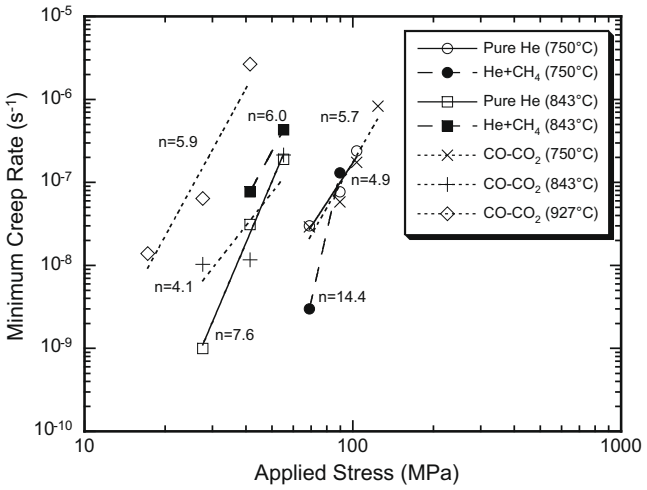

Fig. 5. Stress dependence of creep rate of Alloy 800H tested at 750 °C and 843 °C in pure He, CO–CO_2, and He + CH_4 environments.

where the mobility of dislocations is restricted [18,21,25,26]. This can occur as a result of carbide precipitation in the alloy when tested in the methane containing He environment.

3.2. Failure modes in creep

Fractographic analysis was conducted to characterize the failure modes in specimens tested in He and He + CH_4 environments. Fig. 6 shows the creep fracture morphology of Alloy 800H tested at 750 °C and 68.9 MPa in pure helium environment. It is clear that the fracture mode is transgranular ductile. Fig. 7 shows the fracture surface of a specimen after creep testing at 750 °C and 68.9 MPa in He + CH_4 environment. Fig. 7a indicates a cleavage fracture mode while Fig. 7b is a high magnification image of Fig. 7a clearly illustrating fine cleavage facets. In addition, secondary cracking and void formation are also evident in the photomicrograph. The lower ductility and longer rupture life in methane containing helium environment compared to that in pure helium can be associated with the occurrence of cleavage fracture. Occurrence of cleavage fracture in Alloy 800H in impure helium environments has not been reported in earlier studies [4–7,11] that were conducted at relatively higher pO_2 environments. At higher applied stresses at 750 °C, the difference in rupture life and ductility was not significant between the two environments, and ductile fracture was observed in both pure helium and impure helium environments.

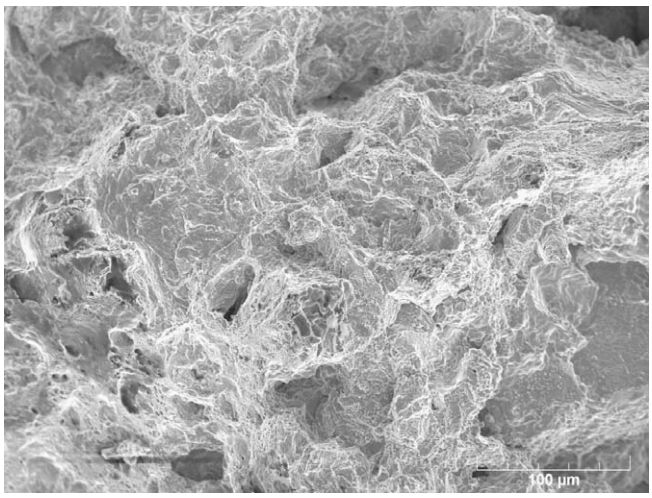

Fig. 6. Ductile fracture behavior of Alloy 800H, after creep testing in pure helium environment at 750 °C, 68.9 MPa.

The fracture morphology at 843 °C and 55.2 MPa is shown in Fig. 8, which indicates a ductile fracture in the helium environment and an intergranular failure in the methane containing helium environment. The intergranular fracture was however, observed only at the corners/edges of the specimen; at the specimen center, a transgranular ductile fracture was observed. It appears that, in He + CH_4 environment, crack initiates intergranularly at the specimen surface. Based on the fractographic observations at 843 °C at all stress levels, it can be said that the fracture mode in He is transgranular ductile, while in the He + CH_4 environment it is mixed intergranular/transgranular. However, due to the higher applied stress, there is no significant difference in the rupture strength and ductility in both the environments at 843 °C, even though the fracture mechanisms may be different.

Preliminary cross-sectional analysis of fractured specimens showed formation of chromia scale (3–5 μm thick) on the specimen surface in both He and He + CH_4 environments. In addition, (Cr,Mn)-spinel phase was also observed in He + CH_4 on specimens tested at lower stresses. However, there was no clear evidence of preferential crack propagation through any second phase particles in either the He or the He + CH_4 environment. Detailed TEM and cross-sectional analysis of failed specimens is warranted to precisely characterize the micromechanisms for cleavage fracture in He + CH_4, and the role of carburization, decarburization, and/or oxidation that occur in He and He + CH_4 environments in the creep performance of the alloy.

The above fractographic characterization indicates that at lower applied stresses, methane in helium affects the deformation behavior and the creep-rupture strength of Alloy 800H. Therefore, it is concluded that a combination of low stresses and a favorable combination of environment is required to initiate cleavage fracture. The authors' previous work [27] on Alloy 617 also demonstrated cleavage fracture at low applied stresses in methane containing helium gas.

The specimens tested in low-pO_2 (1%CO–CO_2) environment exhibited predominantly oxide scales, the composition of which was influenced by the oxygen partial pressure in the exposure environment. Analysis of cross sections of fracture surfaces showed chromium oxide formation with significant internal oxidation.

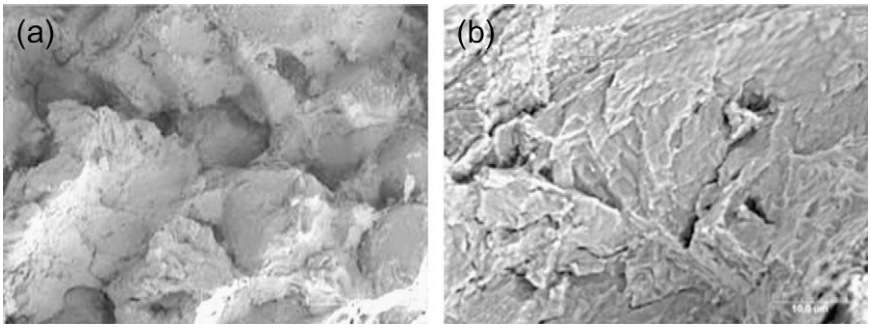

Fig. 7. Brittle fracture in Alloy 800H after creep testing in He plus 675 vppm CH_4 environment at 750 °C, 68.9 MPa in (a) low magnification (b) higher magnification illustrating cleavage facets.

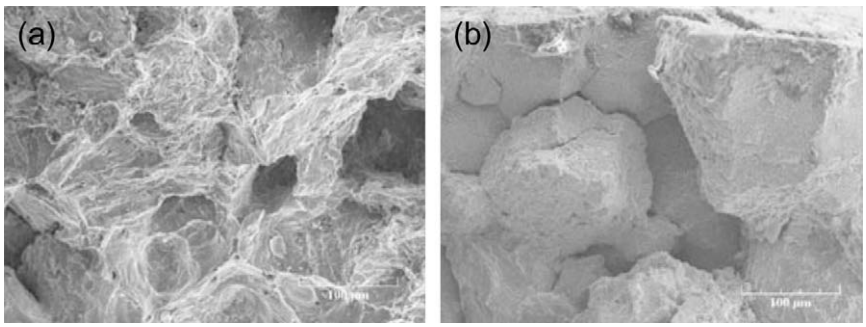

Fig. 8. Effect of methane on the creep fracture modes in Alloy 800H tested at 843 °C, 55.2 MPa. Specimens tested in (a) pure He environment, illustrating ductile fracture and (b) He plus 675 vppm, illustrating cleavage fracture.

4. Summary

A preliminary investigation was conducted to evaluate the creep behavior of Alloy 800H in the temperature range 750–927 °C in impure helium and in low-pO_2 (established by a mixture of 1%CO–CO_2) environments. A helium test facility was set-up that ensured accurate control of the impurities at the required level during the entire duration of the creep tests.

At 750 °C and 68.9 MPa, Alloy 800H exhibits the lowest rupture strain and longest rupture life in He + CH_4 compared to the He environment. The reduction in creep-rupture strain in He + CH_4 is attributed to the occurrence of cleavage fracture. Additional tests are needed to verify the alloy behavior at lower stresses and at lower temperatures. At higher applied stress and also at higher temperatures, the creep-rupture lives and rupture strains in He and He + CH_4 were similar. Furthermore, the creep behavior in the low-pO_2 (1%CO–CO_2) environment was comparable to that observed in the pure helium environment.

Alloy 800H follows a dislocation climb-controlled power-law behavior in He ($n = 6.9$) and low-pO_2 ($n = 5.6$) environments, whereas a different behavior is observed in the He + CH_4 ($n = 9.8$) environment. The apparent activation energies for creep in the He and in 1%CO–CO_2 were 391 kJ/mol and 398 kJ/mol, respectively, whereas it was 723 kJ/mol in the He + CH_4 environment. Furthermore, the activation energy appears to be independent of stress in He and in 1%CO–CO_2 while it seems to be stress dependent in the He + CH_4 environment.

Creep fracture occurs by a transgranular ductile mode in He environment at all applied stresses at both 750 °C and 843 °C in the present study, whereas in the He + CH_4, fracture occurs by cleavage at lower applied stress and at relatively low temperatures. At higher temperatures, the fracture mode was mixed intergranular/transgranular at all applied stresses in the He + CH_4 environment. It is believed that lower stresses and temperatures and a specific gas chemistry condition are needed to initiate cleavage cracking. The results of this study indicate a critical need to establish the performance envelope for Alloy 800H for use in control rods and other components in VHTRs and to specify the purity requirements for the reactor helium for acceptable long-term performance of these component materials in advanced reactors.

Acknowledgments

This work was initiated under the sponsorship of the US Nuclear Regulatory Commission and continued under US Department of Energy contract DE-AC02-06CH11357. The authors thank D.L. Rink for his assistance with microstructural characterization.

References

[1] A Technology Roadmap for Generation IV Nuclear Energy Systems, US DOE Nuclear Energy Research Advisory Committee and the Generation IV International Forum, December 2002.
[2] M. Cappelaere, M. Perrot, J. Sannier, Nucl. Technol. 66 (1984) 465.
[3] W.R. Johnson, G.Y. Lai, Interaction of Metals with Primary Coolant Impurities: Comparison of Steam-Cycle and Advanced HTGRs, Report IWGGCR-4, IAEA Specialists Meeting on High Temperature Metallic Materials for Application in Gas-Cooled Reactors, 1981, Paper J1.
[4] L.W. Graham, J. Nucl. Mater. 171 (1990) 76.
[5] H.M. Yun, P.J. Ennis, H. Nickel, H. Schuster, J. Nucl. Mater. 125 (1984) 258.
[6] K.S. Lee, Nucl. Technol. 66 (1984) 241.
[7] F. Schubert, Evaluation of Materials for Heat Exchanging Components in Advanced Helium-Cooled Reactors, IWGGCR-9, Specialists' Meeting on Heat Exchanging Components of Gas-Cooled Reactors, 1984, pp. 309–334.
[8] K. Natesan, A. Purohit, S.W. Tam, Materials Behavior in HTGR Environments, NUREG/CR-6824/ANL-02/37, 2003.
[9] W. Betteridge, R. Krefeld, H. Krockel, S.J. Lloyd, M. Van de Voorde, C. Vivante (Eds.), Proc. Conf. on Alloy 800, Petten, The Netherlands, March 14–16, North-Holland Publishing Company, Amsterdam, 1978.
[10] G.O. Hayner, R.L. Bratton, R.N. Wright, W.E. Windes, T.C. Totemeier, K.A. Moore, W.R. Corwin, T.D. Burchell, J.W. Klett, R.K. Nanstad, L.L. Snead, Y. Katoh, P.L. Rittenhouse, R.W. Swindeman, D.F. Wilson, T.E. McGreevy, W. Ren, Next Generation Nuclear Plant Materials Research and Development Program Plan, INL/EXT-05-00758, 2005.
[11] P.J. Ennis, K.P. Mohr, H. Schuster, Nucl. Technol. 66 (1984) 363.
[12] D.I. Roberts, Design codes and lifetime prediction aspects for alloy 800 for nuclear and non-nuclear applications, in: Proc. Intl. Conf. on Alloy 800, J.R.C. Petten Establishment, Petten, The Netherlands, North Holland, 1978, p. 403
[13] M.K. Booker, V.B. Baylor, B.L.P. Booker, Survey of Available Creep and Tensile Data for Alloy 800H, ORNL/TM-6029, 1978.
[14] O.D. Sherby, P.M. Burke, Prog. Mater. Sci. 13 (1967) 325.
[15] K. Natesan, W.K. Soppet, A. Purohit, J. Nucl. Mater. 307–311 (2002) 585.
[16] M.E. Kassner, M.T. Perez-Prado, Prog. Mater. Sci. 45 (2000) 1.
[17] R.W. Hertzberg, Deformation and Fracture Mechanics of Engineering Materials, fourth ed., John Wiley and Sons Inc., 1996.
[18] L. Kloc, Sklenicka, A. Dlouhy, K. Kucharova, in: A. Strang, D.J. Gooch (Eds.), Microstructural Development and Stability in High Chromium Ferritic Power Plant Steels, No. 2, The Institute of Materials, 1998, p. 445.
[19] F.H. Norton, The Creep of Steel at High Temperatures, McGraw-Hill, NY, 1929. p. 124.
[20] T.G. Langdon (Ed.), Dislocations and properties of real materials, in: Proc. Conf. Inst. Metals, London, 1984, p. 221
[21] J.E. Bird, A.K. Mukherjee, J.E. Dorn, in: D.G. Brandon, A. Rosen (Eds.), Quantitative Relation Between Properties and Microstructure, Israel University Press, Jerusalem, 1969, p. 255.
[22] J. Weertman, Trans. ASM 61 (1968) 681.
[23] J.T. Guo, C. Yuan, H.C. Yang, V. Lupinc, M. Maldini, Met. Trans. 32A (2001) 1103.
[24] C.T. Sims, N.S. Stoloff, W.C. Hagel (Eds.), Superalloys II, Wiley and Sons Inc., NY, 1987.
[25] M.S. Soliman, F.A. Mohamed, Metall. Trans. 15A (1984) 1893.
[26] M.S. Soliman, J. Mater. Sci. 22 (1987) 3529.
[27] P.S. Shankar, K. Natesan, J. Nucl. Mater. 366 (2007) 28.